7

Pulse Laser Ablation by Reflection of Laser Pulse at Interface of Transparent Materials

Kunihito Nagayama, Yuji Utsunomiya,
Takashi Kajiwara and Takashi Nishiyama
Kyushu University
Japan

1. Introduction

This chapter is devoted to a series of studies on a peculiar kind of pulse laser ablation which is found to take place at the interface of two transparent materials. Transparent media treated here include air (gas), liquid and solid medium.

This research started from the discovery of appreciable reduction of laser ablation threshold for roughened solid surface by our group. (Nagayama et al, 2005) As will be explained later in detail, precise study on this phenomenon revealed that

i. peculiar effects are observed for the interface of transparent and roughened solid surface,
ii. the phenomena have no appreciable dependence on the surface roughness,
iii. the phenomena depend strongly on the direction of the incident laser beam, i.e., whether the incident beam comes from the material of higher refractive index to that of lower one.
iv. this effect is not a microscopic one, but a macroscopic one,
v. since the phenomenon can be qualitatively described by optics equations.

Appreciable enhancement of laser absorption or the reduction of ablation threshold occurs only when the laser beam is incident from the material of higher refractive index to that of lower index. In other words, the phenomena are represented by the difference in refractive index of adjacent media in both sides of the material interface, and not by the mechanical properties of media.

This chapter consists of three topics, which are (i) the enhancement of laser beam absorption by roughened surface, and its evidence through high speed imaging of the ground glass surface ablation, and its unique application to the initiation of high explosive powder (Nagayama et al, 2005, 2007, 2007a), (ii) after a simple theoretical discussions on physics involved in the phenomena, pressure wave generation from material interface of glass or PMMA surface in air or in water, and its high speed imaging, (Nakahara et al, 2008) are described and finally, (iii) liquid jet formation from liquid-air surface will be described. (Utsunomiya et al, 2009, Kajiwara et al, 2009, Utsunomiya et al, 2010) Key issue of the physics involved in all the phenomena treated in this chapter is the difference in refractive index of a transparent material from that of the adjacent medium.

2. Reduction of pulse laser ablation threshold fluence for roughened surface of a transparent material

2.1 Evidences of enhanced absorption of laser energy at roughened surface

We have found appreciable reduction of pulse laser ablation threshold of transparent materials, when the laser beam is focused through the material to the interface of the material and air, if the output surface is a roughened surface. (Nagayama et al, 2005) Peculialities of ablation of non-smooth surfaces, however, have been reported by several authors. (Ben-Yakar et al, 2003, Kane and Halfpenny, 2000, Petr-Chylek et al, 1986) This effect is striking in that this happens only when the laser beam is focused on the surface of the transparent material not from the air but from inside the material. In other words, the effect is laser direction dependent.

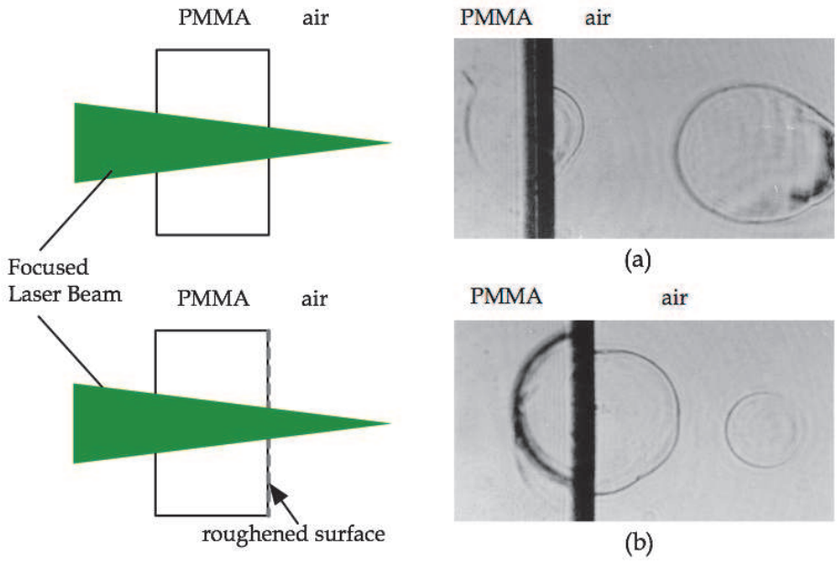

Fig. 2.1 High speed imaging of laser focus into air through PMMA plate with smooth (a) and roughened surface (b). Surface of PMMA was roughened by using #800 paper. Delay time of photos are 0.53 and 0.54 μs, respectively with a focused laser pulse of 180 mJ.

Figure 2.1 shows typical demonstration showing the difference in specific features of laser energy absorption at smooth and roughened surface of a transparent plate through which pulsed laser beam is focused into air ahead of the plate. In order to detect small difference in the change in density, pulse laser shadowgraphy with very small aperture has been adopted. Pulse laser used in these experiments is an Nd:YAG laser of fundamental frequency, and the energy per pulse is around 180 mJ. Pulse duration of the pulse is 4 ns. One may see an air shock wave front produced from the focused point in air. One may also see other waves emanated from the air-PMMA plate interface. Stronger stress wave front in PMMA can be seen in case of roughened PMMA surface. Very weak stress wave in PMMA and in air can still be seen even in case of smooth surface of PMMA. Procedures of observing these phenomena will be discussed in a later section.

Similar experiments are performed for the combination of a silica glass plate in contact with distilled water layer. Figure 2.2 shows the typical results. In this case, pulse laser is focused

into water. For glass plate with smooth surface, one may see weak pressure wave around the beam waist, and also a weak wave from the interface. On the contrary, much larger disturbance is produced in case of roughened glass surface.

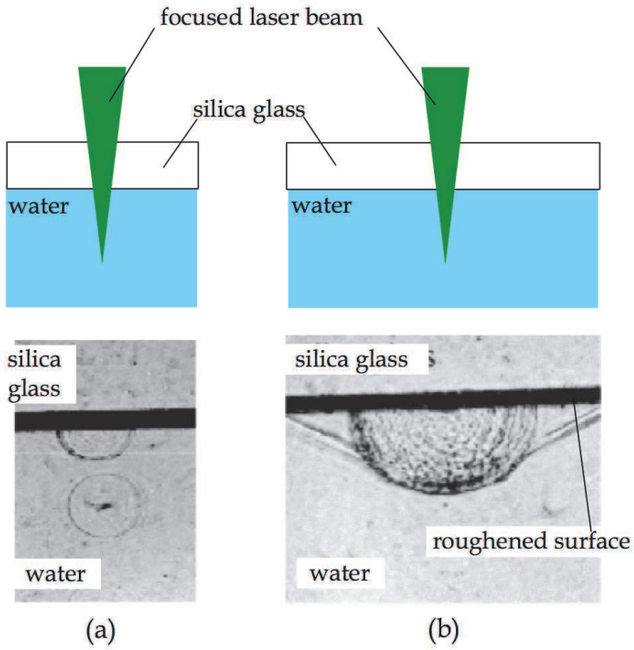

Fig. 2.2 High speed imaging of laser focus into water through silica glass plate with smooth (a) and ground surface (b). Silica glass plate was roughened by #1000 powders. Delay time of photos are 0.56 and 1.0 μs, respectively with a focused laser pulse of 100 mJ.

Two examples shown in Fig. 2.1 and 2.2 suggest the following; (i) roughening treatment of transparent material enhances laser energy absorption resulting in the reduction of ablation threshold, (ii) similar phenomena will take place for two transparent media combination including air-PMMA and water-glass. It is stressed here that direction of laser beam to material interface is from the material of higher refractive index to that of lower one. These results are quite different from the common understanding of pulse laser deposition of thin films. (Chrisey and Hubler, 1994)

In the phenomenon of pulse laser ablation, surface energy density or laser fluence is of essential importance. In this sense, determination of laser fluence must be made very carefully. In case of laser beam with Gaussian profile, it is possible for the fluence at beam waist to calculate theoretically from the value of focal length of focusing lens. In the present study, we have measured energy of incident laser pulse and the cross section of the ablated area in the following way. For the measurement of the ablated surface, we have used the damaged surface area of aluminum plate just in place of the ablation target plane, i.e., at the position of the material interface. Estimated fluence obtained in this manner is normally slightly smaller than those estimated by the theory of Gaussian beam. We used the method throughout this series of studies, since it can be a simple and basically reliable measure of the real fluence value in any situation of the experiments, including in air or in water or in any fluid, applicable for any beam profiles adopted in this study. As is noted later, the present effect has strong dependence on the laser beam pattern.

In this study, three Nd:YAG laser systems with ns duration and of fundamental frequency has been used. One of them (laser #3) was used as a light source for pulse laser shadowgraphy with an SHG crystal. They are summarized in Table 1. First two lasers in Table 1 were used solely for ablation energy source with different beam pattern. Laser #1 can be used altering its beam pattern of near Gaussian and tophat shape by the use of different output mirror. Where tophat pattern means almost uniform beam intensity distribution. Torus shape in Laser #2 indicates intensity distribution with low intensity region in the middle of the beam pattern. They can be synchronized in the precision of less than 20 ns to alter the delay time of taking pictures of the events.

laser #	max energy per pulse	duration	wavelength	beam profile
1	800 mJ	10 ns	1064 nm	Gaussian or Tophat
2	200 mJ	4 ns	1064 nm	Torus
3	200 mJ	7 ns	532 nm (SHG)	Gaussian

Table 1. Nd:YAG laser systems used in this study

2.2 Fragment cloud generation in ground glass ablation

Especially in the case of ground glass, we have observed not only ablation threshold reduction, but also burst of glass fragments from the focused region of the beam. (Nagayama et al, 2007) Figure 2.3 shows high speed imaging of the cloud of fragments burst from the ground surface of glass plate in air. We have used an intensified CCD camera capable of acquiring two frames per one shot. (Hamamatsu C-7972-11) Each frame in Fig. 2.3 corresponds to separate experiments. One notices the reproducibility of the phenomena. One may see a shock front in air followed by burst of material cloud. Appreciable amount of glass fragments are seen to move at high velocity. In most of pulse laser ablation process, material ejection is somewhat a common phenomena normally a final stage of ablation. In case of ground glass ablation, however, amount of material ejection is much larger. This is quite peculiar only in the case of ground glass.

Extensive studies of the ground glass ablation have revealed that (i) the effect has little dependence on the surface roughness, (ii) reduction of ablation threshold fluence is more than ten-fold, (iii) ejected glass particles have the velocity of around 1.5 km/s at least in the initial stage. High-speed glass particle cloud have the ability of initiating high explosive charge, PETN powder. (Nagayama et al, 2007a) We have used special ground glass plates commercially available for optics to diffuse light, called diffusion plates. They are specified by roughness numbers from #240 to #1500.

Figure 2.4 shows high speed imaging of the cloud of fragments burst from the ground surface of glass plate in vacuum. In the figure, it is apparent that air shock precursor does not exist, but still an appreciable amount of fragments can be seen. We have trapped ejected glass particles in a simple setup using two PMMA plates placed at forward and bottom of ground glass target assembly. Figure 2.5 shows particle size distribution for several kinds of diffusion plates with different surface roughness. Two peaks of trapped particle size are observed irrespective of glass surface roughness indicating a scaling law for the physical process of the destruction of brittle materials.

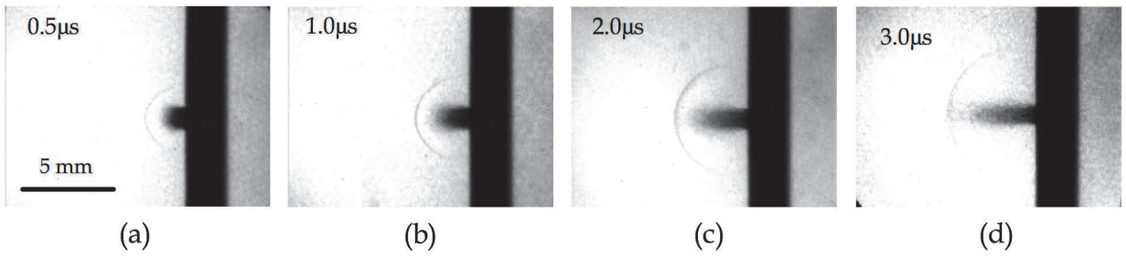

Fig. 2.3 High speed imaging record of glass fragments ejected from the ground glass surface with #240 surface roughness by pulse laser beam focused through the glass plate from right. Delay time of photographs are shown in the figure. Laser energy, focused diameter and fluence are 0.39 J, 1.8 mm, and 15.5 J/cm² , respectively.

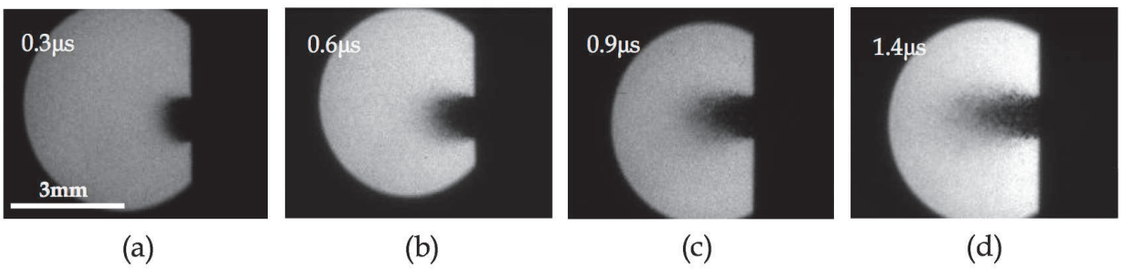

Fig. 2.4 High speed imaging record of glass fragments ejected from the ground glass surface with #240 surface roughness by pulse laser beam focused through the glass plate in vacuum. Delay time of photographs are shown in the figure. Laser energy, focused diameter and fluence are 0.38 J, 1.4 mm, and 25 J/cm² , respectively.

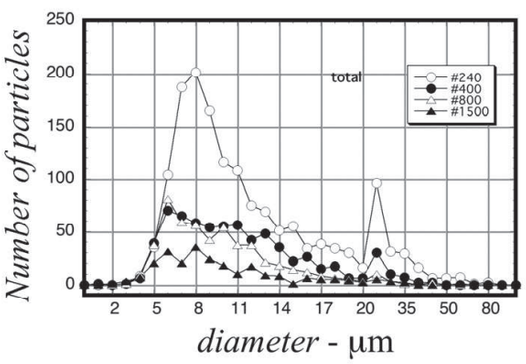

Fig. 2.5 Size distribution of trapped glass fragments from pulse laser ablation of diffusion plates with several different surface roughness (shown in the figure).

2.3 Initiation of PETN high explosive powder by glass ablation

Possibility of applying high velocity particle cloud generation by ground glass ablation to the initiation of high explosive powder has been pursued here. This is supposed to be realized due to the velocity of fragments of 1.5 km/s. We have observed the detonation of PETN powders in two ways. By putting thin PETN powder layers in contact with ground

glass plates with PMMA block, we observed the detonation-induced strong stress wave in PMMA cube by a high-speed camera. (Hamamatsu C-7972-11) Figure 2.6 shows typical records with different delay time. Pulse laser ablation of ground glass induces weak precursor wave followed by higher stress wave in PMMA. They are clearly visible in the photographs in Fig. 2.6. One may note that laser ablation induced wave and detonation induced higher stress wave cannot be seen as one wave but separated. Finite time is seen to be required for the detonation reaction to occur after laser irradiation. This phenomenon is well known by several researchers. (Paisley, 1989, Watson et al, 2000) As one of side evidences on the detonation reaction is the self-emission of detonation-induced plasma in air.

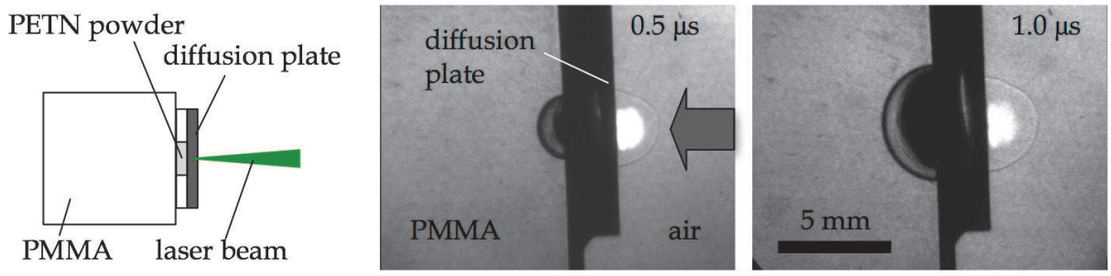

Fig. 2.6 Detonation induced stress wave in PMMA slab by pulse laser ablation of ground glass plate (diffusion plate) with surface roughness of #800 in contact with PETN high explosive powder of initial density of about 1.0 g/cm^3. Delay time of photographs is shown in the figure.

Another kind of experiments was planned to investigate the retardation of detonation reaction after laser irradiation. Since the detonation of PETN powder emits light that can be seen through PMMA cube. Figure 2.7 shows the high speed streak record of self emission by detonation reaction and its propagation to radial direction. It is convenient that pulse laser ablation itself emits light at that instant, this flash is also recorded in streak record. This flash must be the time 0 of the event, and one may see the delay in detonation from ablation.

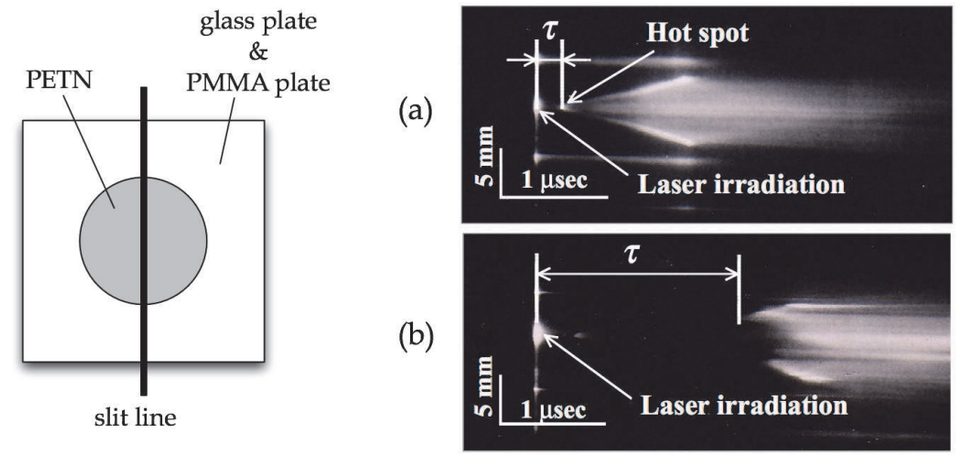

Fig. 2.7 Time sequence of PETN powder initiation experiment. Streak record of self emission by laser ablation and by reaction was obtained by a high-speed streak camera. (Imacon 790) Diffusion plate of #400 was used. Laser fluence is set to (a) 15.1J/cm^2, and (b) 9.1 J/cm^2 , respectively. Ignition delay time τ is defined as in the figure.

Shortest delay time from ablation to detonation is around 200-300 ns, which is almost in harmony with the high speed imaging results as in Fig. 2.6. It is also possible to estimate the detonation velocity by the slope of streak record. Estimated detonation velocity from streak photographs agrees with available data for the detonation velocity of PETN powder of relevant initial density. Streak record in Fig. 2.7 (b) shows the case of incomplete reaction. In such cases, delay time is quite long, and detonation may not be completed.

3. Pressure wave production at material interface by the reflection of focused laser beam

3.1 Possible mechanism of reduction of laser ablation threshold for roughened surface

The key to understand the above-explained phenomena is the fact that they have direction dependence. That is, phenomena expected by laser irradiation are quite different depending upon the direction from which medium to focus through the material interface. Experimental results apparently show that laser beam must be focused through the material of higher refractive index to the interface with that of lower one.

The fact that present phenomena have very weak dependence on the surface roughness of the material suggests that the phenomena is regarded as not a microscopic effect but a macroscopic one. It is plausible that laser beam reflection at the interface between transparent material and adjacent medium must be the key phenomena. That is, difference in refractive index of the transparent material and that of the adjacent medium may lead to the present phenomena. Reduction of ablation threshold in this study can be explained at least qualitatively by Snell's law. (Nagayama et al, 2007, Utsunomiya et al, 2009)

For the reflection of light wave with moderate energy density, Fresnel's equations for the coefficient of reflection r and of transmission t at an interface between two media with refractive indices, n_1 and n_2 are given by

$$r_{\perp} = \frac{n_1 \cos\theta_1 - n_2 \cos\theta_2}{n_1 \cos\theta_1 + n_2 \cos\theta_2}, \quad t_{\perp} = \frac{2n_1 \cos\theta_1}{n_1 \cos\theta_1 + n_2 \cos\theta_2},$$
$$r_{\parallel} = \frac{n_2 \cos\theta_1 - n_1 \cos\theta_2}{n_1 \cos\theta_2 + n_2 \cos\theta_1}, \quad t_{\parallel} = \frac{2n_1 \cos\theta_1}{n_1 \cos\theta_2 + n_2 \cos\theta_1} \tag{1}$$

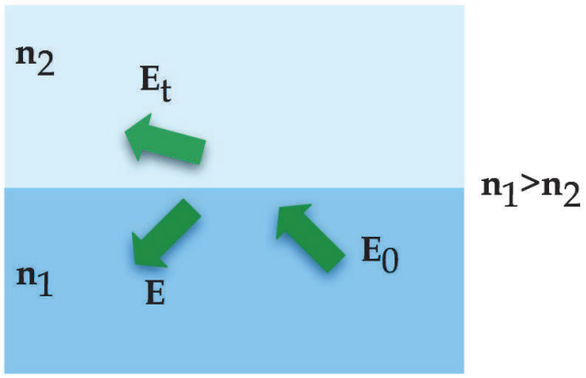

Fig. 3.1 Schematic illustration of the reflection of laser beam at material interface. E_0 and E denote the Electric field strength of the incident beam, and that of the reflected beam.

where suffices ⊥ and ∥ denote light waves whose polarization is perpendicular and parallel to the reflection plane, respectively. Within the light intensities treated here, it is assumed that medium cannot absorb light energy. As for all the variables and notations used here, please refer to the textbook of optics. (Hecht, 1989) By considering the above two kinds of polarizations, one may describe light waves with arbitrary polarization direction. Figure 3.1 shows schematic illustration of electromagnetic wave reflection at a interface of two media with different refractive index.

One may note that how the light reflection at glass-air interface depends on the laser irradiation direction, i.e., from glass to air or from air to glass. Only difference within these two is phase shift by reflection. Important point is the fact that phase shift of reflection at the interface for transmission into medium of lower refractive index is 0. Therefore, the interference between the incident radiation and reflected radiation is **constructive**. In the present case, we have

$$\begin{aligned} E_{\perp} &= E_0 + \frac{n_1\cos\theta_1 - n_2\cos\theta_2}{n_1\cos\theta_1 + n_2\cos\theta_2}E_0 = \frac{2n_1\cos\theta_1}{n_1\cos\theta_1 + n_2\cos\theta_2}E_0, \\ E_{\parallel} &= E_0 + \frac{n_2\cos\theta_1 - n_1\cos\theta_2}{n_1\cos\theta_2 + n_2\cos\theta_1}E_0 = \frac{2n_1\cos\theta_1}{n_1\cos\theta_2 + n_2\cos\theta_1}E_0, \end{aligned} \tag{2}$$

By using Snell's law,

$$n_1 = n_2\frac{\sin\theta_1}{\sin\theta_2} \tag{3}$$

Eq.(2) can be rewritten to

$$\begin{aligned} E_{\perp} &= \frac{2\sin\theta_1\cos\theta_1}{\sin\theta_1\cos\theta_1 + \sin\theta_2\cos\theta_2}E_0, \\ E_{\parallel} &= \frac{2\sin\theta_1\cos\theta_1}{\sin\theta_1\cos\theta_2 + \sin\theta_2\cos\theta_1}E_0, \end{aligned} \tag{4}$$

From Eq. (4), electric field intensity at the material surface has dependence on the incident angle. Maximum field intensity enhancement is obtained for the incident angle of critical value for total internal reflection. In this case, maximum field intensity is two times that of incident field strength. We have to consider the surface energy density at the material interface, so that electromagnetic energy intensity per unit area must be four times that of initial one. On the contrary, it is shown that for light waves incident from the material with lower refractive index, superposed field of incident and reflected wave is **destructive**, so that enhancement of electromagnetic energy density does not happen.

These considerations can explain the effective reduction of ablation threshold fluence and also the direction dependence of the phenomena. Theoretical treatments based on the Fresnell's equations apparently lack the effect of laser absorption by the medium and also non-linear electromagnetic energy density realized by high fluence of focused laser beam. Quantitative explanation of the effect must be made by a theory containing the nonlinear effects of the phenomena and laser energy absorption by the material. Almost same discussion has been made by Greenway et al. (Greenway et al, 2002) Their discussion is

limited to the case of normal incidence and glass-air interface due to their research topics on energy transmission by an optical fiber.

3.2 Evidence on reduction of laser ablation threshold for oblique incidence on material interface

If the above discussion is the case, one can observe the reduction of ablation threshold for the oblique surface of the transparent material prism, if the laser beam is focused through the transparent prism as shown schematically in Fig. 3.2(a). To show the ablation threshold reduction at the interface, we made an experiment using glass prism specimen. Laser fluence at oblique glass surface is set smaller than known ablation threshold. Focused laser beam is incident as shown in Fig. 3.2(a) so as to have a focus at a point inside the glass prism but after reflected at the oblique surface.

As shown in the pulse laser shadowgraph picture in Fig. 3.2(b), one observes air shock front emanated from the point of laser beam reflection. This experimental result and further similar experiments showed that reduction of ablation threshold really takes place at the material interface of two media with different value of refractive index. (Nakahara et al, 2008) Laser beam must be incident from the material of high refractive index for the present effect to occur. In Fig. 3.2(b), incident beam fluence at prism surface is 17 J/cm^2, and that at reflected prism surface is estimated to be 12 J/cm^2. One may note that incident beam is focusing from the incident surface to the oblique surface, but the cross section of the reflected area is larger than the incident area due to elliptical shape of the reflected area. Fluence of the reflected area is appreciably lower than the ablation threshold of this glass in the present pulse laser system of around 20 J/cm^2. We have observed similar phenomena for two materials combination of glass-air, glass-water, PMMA-air and PMMA-water.

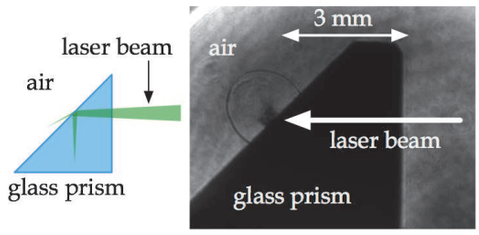

Fig. 3.2 Demonstration experiment showing the reduction of laser ablation threshold by the reflection of laser beam at oblique material interface of glass and air. Estimated laser fluence at oblique surface is appreciably smaller than the measured value of ablation threshold.

In order to obtain further evidences on thershold fluence reduction, we have performed two different experiments. Figure 3.3 shows the experimental observation of pressure wave production at glass prism-water interface by using experimental assembly of Fig. 3.3 (a). In this case, estimated laser fluence at the reflected area is about 7 J/cm^2, which is smaller than threshold fluence of glass. One may note superposition of tiny waves emanated from the beam reflection area. In this case, incident angle of the beam onto the interface is less than the critical angle of total internal reflection between glass and water, transmitted wave induces cavitation bubbles on its way to the focused point. Even so, one may see generation of many waves at reflected interface.

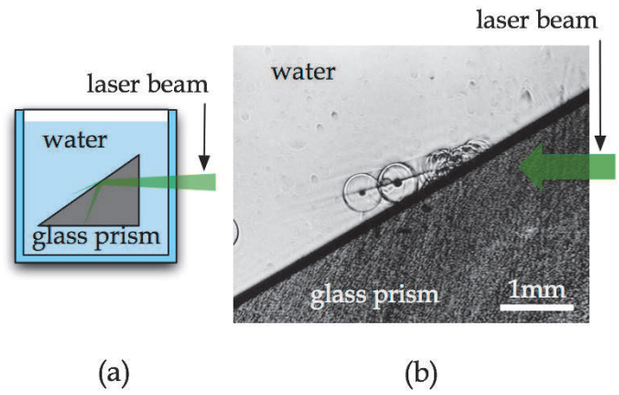

Fig. 3.3 Demonstration experiment showing the reduction of laser ablation threshold by the reflection of laser beam at oblique material interface of glass immersed in water. Estimated laser fluence at oblique surface is smaller than the measured value of ablation threshold.

Reproduction of evidences for the reflection induced ablation is shown in Fig. 3.4. In this case, laser beam is incident on the material interface perpendicularly. Therefore, the field enhancement is not very large, but threshold fluence reduction for ablation can be seen in the figure. This is the case where Greenway et al observed for their optical fiber experiment. These observations lead us to the conclusion that the present effect can be extended to various combination of transparent materials.

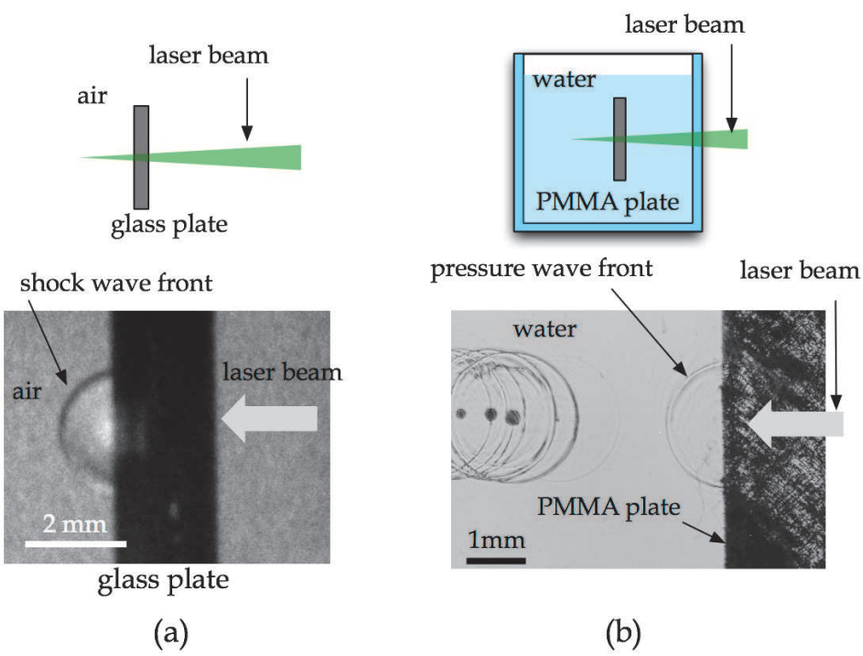

Fig. 3.4 Demonstration experiment showing the reduction of laser ablation threshold by the reflection of laser beam at material interface of glass-air and PMMA immersed in water. Estimated laser fluence at reflected surface is smaller than the measured value of ablation threshold.

4. Liquid jet production at liquid-air interface

4.1 Motivation of experiments on fluid media combination

For medical applications, various activities have reported in the breakdown or ablation of liquids. (Vögel and Venugopalan, 2000, Sigrist, 1986) Natural extension of the present study leads us to the combination of two transparent fluid media. (Utsunomiya et al, 2009, 2010, and Utsunomiya, 2010a) It is expected that at least ablation threshold reduction must be realized even in the case of fluid combinations. We also expect further events of dynamic flows induced by ablation inherent to the properties of fluids. There must also be a general rule of events for any fluid combination irrespective of various material properties such as reactivity, viscosity, etc.

As one of fundamental fluid combinations, we have made extensive studies on the water-air interface ablation by using a very simple assembly of Fig. 4.1. Point of focus of the laser beam is chosen away from the water surface in order to avoid mixing of the breakdown flash at the laser focus and the expected flash from ablation at the water surface. Also in this case, laser beam is lead so as to the water surface and reflected back to the focal point as shown in Fig. 4.1.

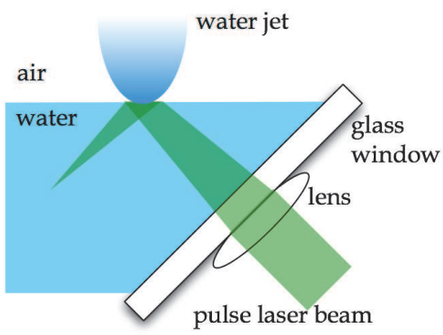

Fig. 4.1 Concept of experimental assembly for fluid experiment.

4.2 Precision pulse laser photography by using high-resolution film with pulse laser light source

We have started the experiments using high speed imaging system by an intensified CCD system. Soon, we have noticed that the phenomena can be recorded only by the system capable of recoding the phenomena with much higher spatial resolution. For this purpose, we have chosen high-resolution film together with pulse laser shadowgraphy. Photographic film we have used is the Minicopy film supplied by FUJI Film Co., Japan. This black and white film has the specifications of 850 lp/mm for 35 mm frame with ASA 25. The only disadvantage of the film is its high contrast of the recorded images. Recorded images are stored in computer by using the film scanner with maximum reading resolution of 12,800 dpi.

We needed at least two pulse laser systems for the ablation energy source and for the light source of photography. We used three Nd:YAG laser systems with 4-10 ns duration and with fundamental frequency. SHG is used only in the case of light source. Figure 4.2 shows diagram of photographic assembly. An aperture is inserted to the objective lens system for the film box to eliminate the flash from ablation and to record the image as shadowgraphs.

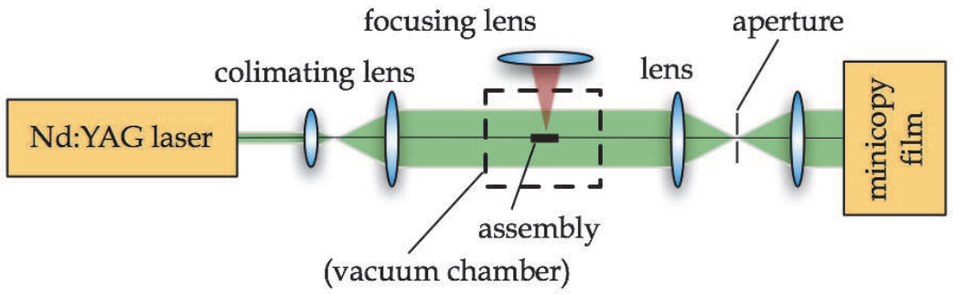

Fig. 4.2 Pulse laser shadowgraphy schematic.

4.3 Water jet generation and evolution

Figure 4.3(a) shows typical pulse laser shadowgraphs representing generation of liquid jet induced by laser ablation of water surface using the assembly of Fig. 4.1. In Fig. 4.3(b), one may also see laser induced cavitation bubble in water by focusing laser pulse from air to inside water.

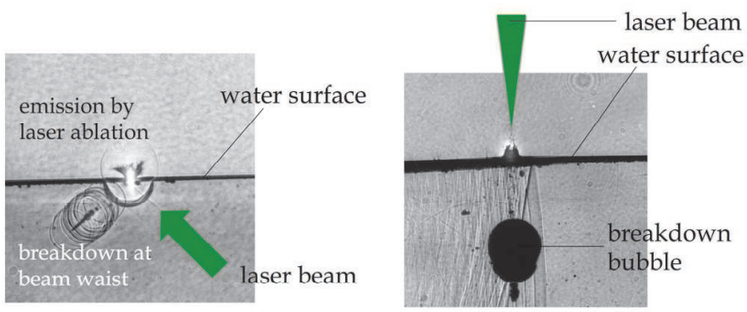

Fig. 4.3 Reproduction of pulse laser shadowgraphs of (a) laser ablation of water surface by using target assembly, Fig. 4.1, and (b) laser ablation induced bubble in water focused from air. Laser fluence on water surface is (a) 25 J/cm^2 and (b) 190 J/cm^2. To observe waves induced by laser ablation or breakdown at water surface or in water, a small aperture in Fig. 4.2 is used.

One may note that the value of fluence at water surface in (a), 25 J/cm^2 and in (b), 190 J/cm^2 is quite different almost one order of magnitude. This is another example of clear dependence of laser ablation threshold on the laser irradiation direction. That is, laser ablation is found to be much easier only in the case of laser irradiation from inside water to air interface. As is seen in Fig. 4.3(a), one may see that pressure waves are produced both at water surface and at beam waist of focal region after laser reflection at water surface. These waves are separated spatially and at least at this delay time, they do not interact with each other, indicating that these waves are the results of independent events. Phenomenon after laser ablation of liquid surface is also laser direction dependent. The value of laser ablation fluence, 25 J/cm^2 is almost two times larger than those obtained in cases of solid materials. It is emphasized that laser ablation of liquid materials is, in our experience, more difficult than of solid materials.

Laser ablation induced dynamic phenomena for liquids are quite different from those for solid materials. Temporal behaviour after ablation is shown in Fig. 4.4. In this sequential display of photographs, we have used three different laser conditions with different beam patterns, which are (a) tophat, (b) Gaussian, and (c) torus shape. Laser #1 and 2 in Table 1 are used in these experiments. As is seen in the figure, liquid jet and its evolution strongly depend on beam profile. Unfortunately, laser #2 has smaller output energy and this makes the phenomena smaller and faster. We noticed that the phenomena depend on (i) laser fluence, (ii) beam profile, and (iii) spot size at water surface. Since the product of laser fluence and spot size gives incident laser energy, parameter (iii) can also be replaced by laser energy.

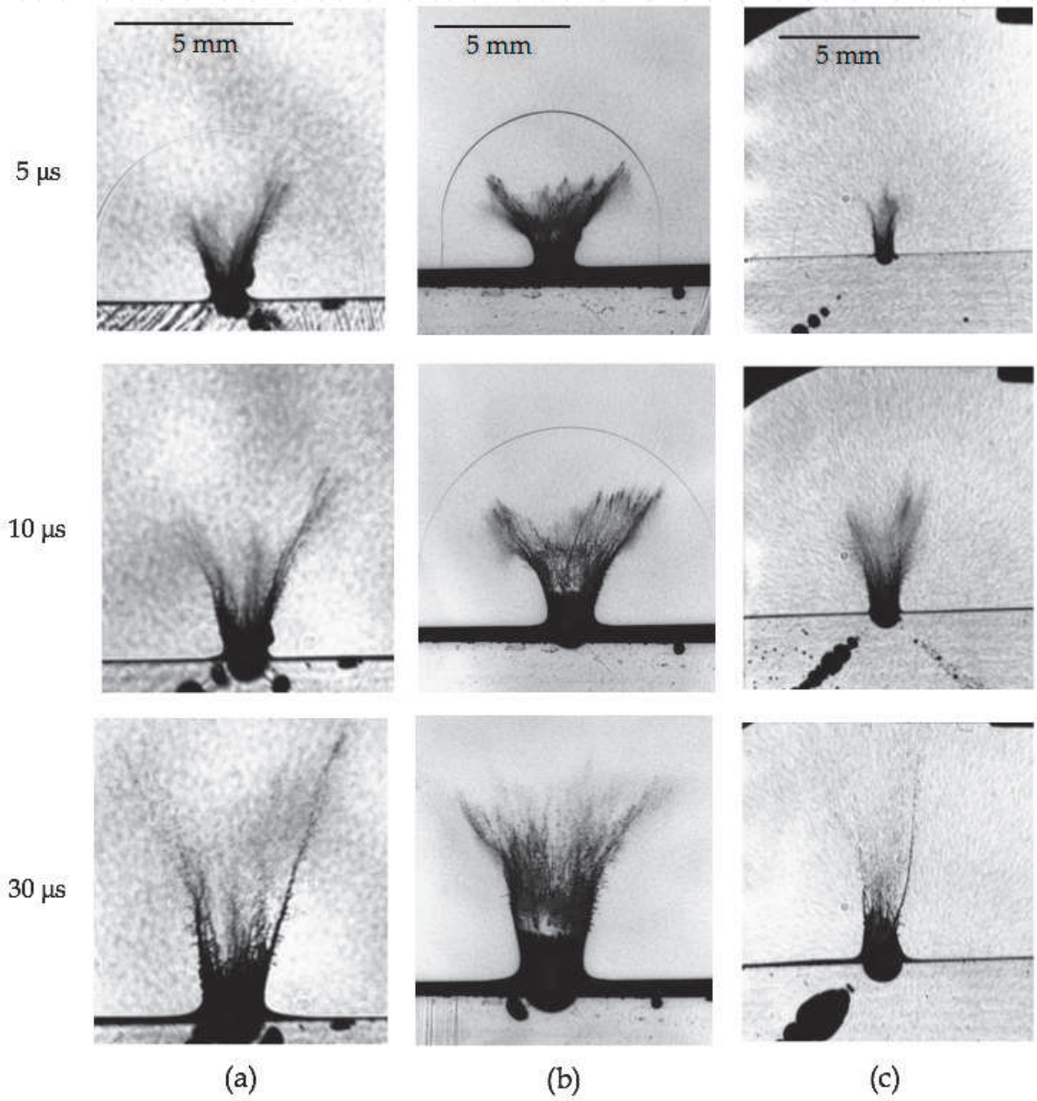

Fig. 4.4 Jet production by water surface ablation by focusing laser beam in water reflected at the surface and to a focus in water. Delay time of these pictures are given left side of pictures. Beam pattern used are (a) tophat, (b) Gaussian, and (c) torus shape, respectively. Laser fluence and energy of each series of experiments are (a) 30 J/cm^2, 300 mJ/pulse, (b) 20 J/cm^2, 300 mJ/pulse, and (c) 25 J/cm^2, 62 mJ/pulse, respectively.

From the photographs, one may see that air shock is followed by a bunch of slender water jet as a form of ligaments from the water surface. By taking successive photographs of jet propagation, one may see that ligament will elongate with time to disintegrate at the tip into droplets. Atomized water particles can be recorded even in these photographs in Fig. 4.4.
It is shown that liquid jet has the velocity of around 1 km/s at the initial stage but slows down very rapidly associated with atomization. Jet production behaviour is found to be dependent strongly on the laser beam profile as well as laser fluence. (Utsunomiya et al, 2010) Tip of liquid ligaments is found to slow down very rapidly. This result can be explained by very fast disintegration of ligaments into small liquid droplets. It is plausible that small droplets themselves will slow down very rapidly due to air drag. In this sense, liquid jet does reach finite distance depending on experimental parameters. In the end, small liquid droplets will evaporate to liquid vapour, and vapour molecules may diffuse into air. These considerations lead to the conclusion that after the liquid jet reaches its maximum height, very slow process of jet and liquid droplets and liquid vapour will be expected.

4.4 Dependence of water jet generation on various parameters

Most of the pulse laser ablation process is governed by so-called laser fluence on the focused target surface. Above the threshold fluence, explosive burst of electrons, ions, atoms, molecules and clusters of the target materials takes place. In the case of liquid surface ablation, however, further dynamics will follow after these material burst. They are dynamic liquid flow induced by instantaneous high plasma pressure of the ablated liquid. Air shock precursor wave, high-speed liquid ligament extension, disintegration into droplets, evaporation, etc. All these dynamics except for the initial burst may be scale dependent, i.e., they will depend on the focused beam size on the liquid surface, since plasma volume is given by this size.
As noted earlier, liquid surface ablation in this study is found to be dependent not only on laser fluence but also on laser energy with keeping fluence constant. We then planned to make experiments with varying fluence, energy and beam pattern systematically. We chose the tophat beam pattern as a standard, and compare the results of other profiles with that of tophat configuration. As shown in Fig. 4.4, it is found that water surface ablation takes place with laser fluence larger than 20 J/cm^2. We have performed systematic experiments for three beam patterns by varying fluence in order to determine the threshold fluence for ablation. Threshold fluence of ablation is almost independent of beam pattern and is 20-25 J/cm^2. The value is also independent of incident laser energy in the interval of 50 mJ/pulse to 400 mJ/pulse.
Increase in laser fluence leads to the occurrence of breakdown along incident beam path toward water surface. Appreciable incident laser energy is absorbed until beam reaches the water surface. As a result, part of the incident laser energy is used to produce cavitation bubbles along incident beam path.
Dependence of ablation behaviour on the laser beam pattern can be seen in Fig. 4.4. In fact, the fastest velocity of ligament tip is obtained in the case of Gaussian beam, and the slowest one is in the case of torus beam. Difference in the ablation behaviour on the beam pattern is attributed to the spatial distribution of local fluence on the water surface due to beam profile. It is also plausible that the difference in the coefficient of absorption of laser energy above the threshold fluence may not be linear to the difference of fluence from the threshold value.

Ablation behaviour depends on the incident laser energy itself as well as laser fluence, i.e., surface energy density. This is a peculiar characteristic of fluid ablation, since almost all of the solid surface ablation must be determined solely by the fluence. As is stated earlier, larger spot size on the water surface creates larger number of ligaments, thereby larger and longer dynamic flow of water.

4.5 Water surface ablation in various geometries

We have also tried water surface ablation experiments in various geometries. Figure 4.5 shows some of the results of these kinds of experiments. We first tried slant water surface by a glass plate with small opening and is ablated by a laser pulse focused in horizontal direction as shown in Fig. 4.5(a). Next, we tried to ablate a part of air bubble created in water, and is ablated to generate slender jet inside the bubble as shown in Fig. 4.5(b). In both cases, water surface is curved by surface tension. The last example is the behaviour of two bubbles by the pulse laser ablation as shown in Fig. 4.5(c). These two bubbles are near enough to interact with each other after ablation. Bubble breakup, or smaller bubble production, is observed depending on the number of bubbles, and their spatial position relative to the focused laser beam.

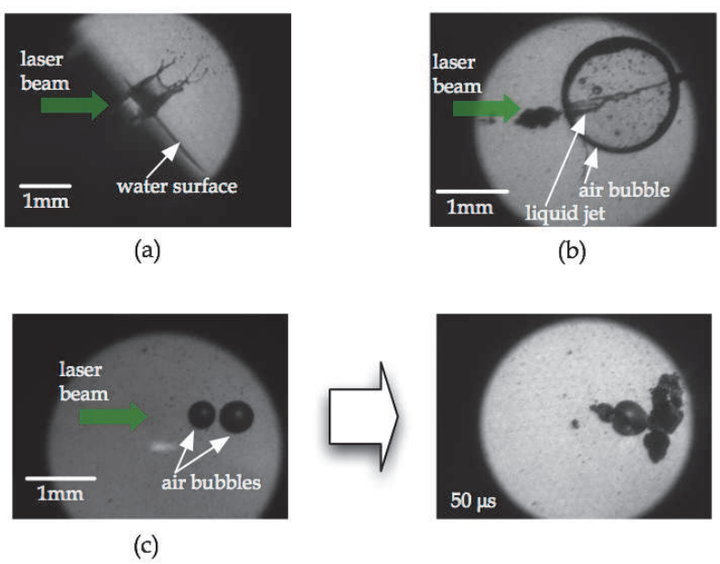

Fig. 4.5 Surface ablation in various geometries. (a) oblique water surface, (b) liquid jet inside air bubble, and (c) bubble collapse by laser ablation.

4.6 Ablation of various liquid samples

We have investigated laser ablation behaviour of several liquid samples other than water. Sample materials tested in this study include ethanol and vacuum oil. Further flammable materials were also tested, since the ablation produces cloud of small droplets or vapour that can be ignited by some means. All of the flammable materials can be ablated and are possible to ignite by a heated wire. Ignition, however, requires large delay time probably due to the fact that atomized or evaporated liquid vapour may reach the place of heated wire with very slow velocity.

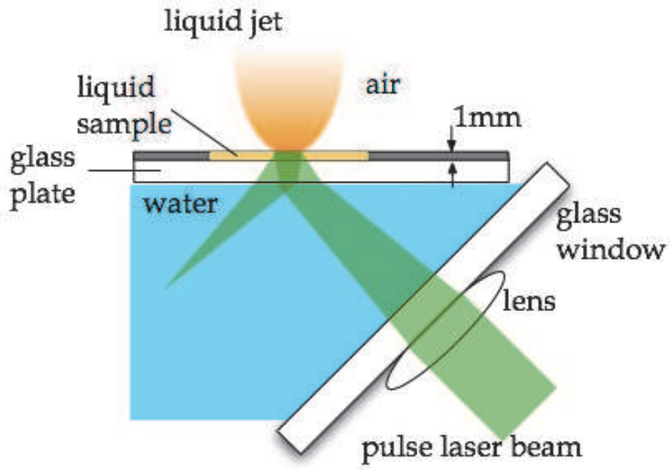

Fig. 4.6 Thin liquid film assembly for energetic liquid samples.

We have used a different sample assembly from that used for water. Schematic illustration of the assembly is shown in Fig. 4.6. Liquid sample is used in the form of a thin layer on glass substrate, which is placed on a water vessel. Laser beam is led from bottom right to the water vessel through the glass plate and to the thin sample. This assembly structure is adopted by the following reason. Since precise specification of the exact laser fluence at the liquid sample surface is essential in this study, the distance from the focusing lens to the sample surface must be precisely controlled and fixed. At least for ethanol sample, constant evaporation from the ethanol surface prevents from precise control of the above distance in the previous assembly in Fig. 3.1. By the use of the assembly in Fig. 4.6, only small amount of sample is set to the sample section and pulse laser is shot before they are about to dry out. We also found that if the laser beam is incident to the assembly from the angle for total internal reflection for water and not for sample, angle of reflection on the sample surface is automatically equal to the critical angle of total internal reflection between the sample and air.

In order to check the usefulness of this setup, we have also observed the ablation behaviour of water samples and compared the results with those for other liquid samples. Figure 4.7 shows reproduction of observed ablation and jet behaviour of water, ethanol and vacuum oil. These three liquid samples are quite different in properties of viscosity and vapour pressure. Very high viscosity and very low vapour pressure for vacuum oil is the reason why we chose this material as a liquid specimen. Table 2 summarizes typical material properties of these materials.

As stated in the previous section, ablation threshold for these materials are almost the same, so that the same experimental conditions are used for each experiment. Comparison of the photographs of Fig. 4.7 shows that among three liquids, ethanol ablation induces mist-like particle cloud and no appreciable generation of ligaments, while ligament-like structure is kept for a long time in the case of vacuum oil. These differences are attributed to the difference in their material properties. Compared with water jet, extension of ligaments for vacuum oil is shorter and the disintegration or atomization delays. One may note a hump

just right of jet especially in the later frame of the photographs indicates an influence of thin film sample structure in this assembly.

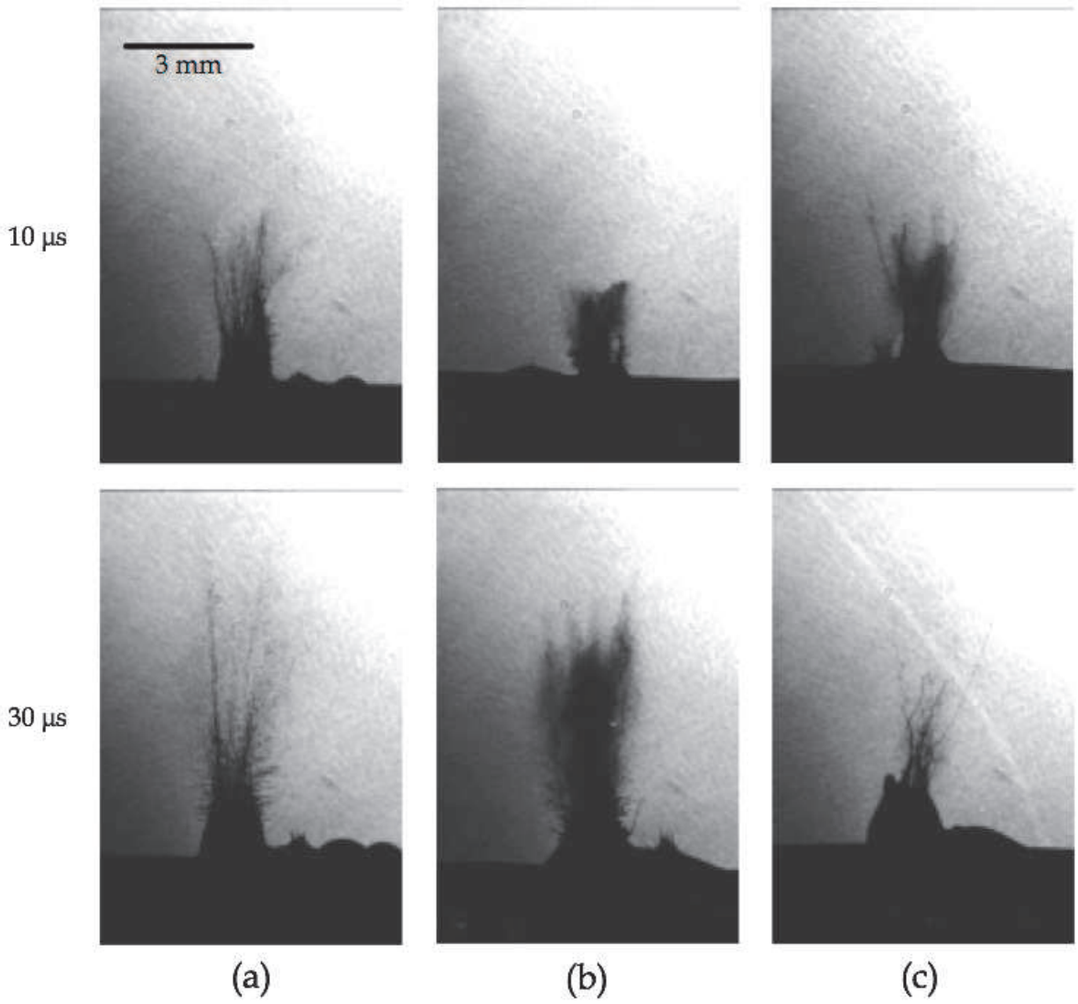

Fig. 4.7 Jet behavior of liquid specimens using assembly of Fig. 4.6. Liquid samples used are (a) : water, (b) : ethanol and (c) : vacuum oil.

sample	initial density (g/cm^3)	viscosity (mPa•s)	vapour pressure (mmHg)
water	1.0	0.89	24
ethanol	0.8	1.2	59
vacuum oil	0.9	23	$7.5X10^{-9}$

Table 2. Material properties of liquid samples

5. Summary and conclusion

Present study shows two extremely different threshold fluence for pulse laser ablation for transparent materials depending on the direction of laser incidence on the material interface. Let us summarize these two threshold fluences. Threshold fluence for transparent materials must be very high easily inferred from the very low absorption of light energy at least for low laser intensity. Experience showed that threshold fluence for ground glass surface through the glass is almost one order of magnitude lower than that for direct laser focus from air. Smallest laser fluence for ground glass surface in this study is about a few joules per square centimeter. Typical and minimum fluence for pulse laser ablation of various material surface are summarized as

2-5 J/cm² : normal incidence, air, roughened PMMA surface
10 J/cm² : normal incidence, air, smooth PMMA surface
1-3 J/cm² : normal incidence, air, roughened glass surface
20 J/cm² : normal incidence, air, smooth glass surface
6-10 J/cm² : oblique incidence, water, smooth glass surface
12 J/cm² : oblique incidence, air, smooth glass surface
20-25 J/cm² : oblique incidence, air, surface of all liquid samples

These values may vary depending on the laser system. That is, pulse duration and beam profile, in other words, instantaneous irradiance and its spatial distribution over the focused area. For the case of transparent fluid media, little information for ablation threshold has been known. Threshold fluence for fluids is found to be almost two times larger than that for solid transparent materials.

Pulse laser ablation of transparent materials is found to be special in that from which direction the focused laser beam is incident determines the behaviour. As explained earlier, they are relevantly but only qualitatively described by the optics equations. Gross reduction of ablation threshold fluence for roughened surface of transparent materials can also be described by the same physics. Surface ablation of transparent solids and furthermore, that of transparent liquids can also be described by the same theoretical basis.

Ground glass ablation produces high velocity glass fragments cloud that can be successfully applied to the initiation of small amount of high explosive powder. Ablation of roughened PMMA plate in water produces pressure pulse, and that can be produced repetitively. This phenomenon will be applied to controllable medical tools in microsurgeries. Ablation of liquid surface produces high-speed liquid jet and eventually produces small droplet cloud. High-speed liquid jet can be used as an injector in medical area. In order to realize usable liquid jet, jet must be shaped as a convenient straight slender jet. Artificial laser beam profile must be used for this purpose, as seen in the dependence of the phenomena on beam profile. We observed very slender jet in air bubble due to the curvature of bubble surface, which has similar effect as the beam profile.

6. Acknowledgment

Authors wish to thank graduate students and undergraduate students involved in these projects especially in experimental activities. They are also indebted to the support of Mr. Tamio Iwasaki of Nobby Tech. Ltd. for high speed imaging, and Ms. Mariko Murakami for

arranging laser instrumentation. Part of the present work was supported financially from the Ministry of Education, Culture and Science, Japan.

7. References

Ben-Yakar,A., Byer,R.L., Harkin,A., Ashmore,J., Stone,H.A., Shen, M., Mazur, E. (2003), *Morphology of femotosecond-laser-ablated borosilicate glass surfaces*. Appl. Phys. Lett. Vol. 83, pp. 3030–3032

Chrisey, D.B., and Hubler, G.K. (1994), *Pulse Laser Deposition of Thin Films* (Wiley, New York)

Greenway, M.W.,Proud, W.G.,Field, J.E.(2002), *The development and study of a fiber delivery system for beam shaping*. Rev. Sci. Instrum., Vol. 73, (2002), pp. 2185–2189.

Hecht, E. (1989), *Optics*, (Addison-Wesley), p.94

Kajiwara, T., Utsunomiya, Y., Nishiyama, T., Nagayama, K. (2009), *Generation of Energetic Liquid Jet and Atomization by Pulse Laser Reflection at Inclined Surface of High Refractive Index Material*, Sci. Tech. Energetic Materials, Vol.70, No.4, (2009), pp. 105-108.

Kane, D.M., Halfpenny, D.R.: *Reduced threshold ultraviolet laser ablation of glass substrates with surface particle coverage: a mechanism for systematic surface laser damage*, J. Appl. Phys. 87, 4548–4552 (2000)

Nagayama, K.; Kotsuka, Y., Nakahara, M., and Kubota, S., (2005), *Pulse laser ablation of ground glass surface and initiation of PETN*, Sci. Tech. Energetic Materials, Vol.66, No.6, (2005), pp. 416-420.

Nagayama, K.; Kotsuka, Y., Kajiwara, T., Nishiyama, T., Kubota, S., Nakahara, M. (2007), *Pulse laser ablation characteristics of quartz diffusion plate and initiation of PETN*, Sci. Tech. Energetic Materials, Vol.68, No.3, (2007), pp. 65-72.

Nagayama, K., Kotsuka, Y., Kajiwara, T., Nishiyama, T., Kubota, S., Nakahara, M. (2007a), *Pulse Laser Ablation of Ground Glass*, Shock Waves, Vol.17, (2007), pp. 171-183.

Nakahara, M., Nagayama, K., Kajiwara, T., and Nishiyama, T. (2008), *High-Speed Photographic Observation of Shock-Pressure Pulse in Water Induced by Laser Energy Absorption at Roughened Surface*, Material Science Forum, Vol. 566 (2008) pp. 47-52.

Paisley, D.L.(1989), *Prompt detonation of secondary explosives by laser*, Proc. 9th Int. Symp. Detonation, (1989) pp. 1110–1117.

Petr Chylek, M.A. Jarzembski, Chou, N.Y.(1986), *Effect of size and material of liquid spherical particles on laser-induced breakdown*. Appl. Phys. Lett. Vol. 49, pp. 1475–1477

Sigrist, M.W. (1986), *Laser generation of acoustic waves in liquids and gases*, J. Appl. Phys. Vol. 60, pp. R83-R122

Tominaga, T., Nakagawa, A., Hirano, T., Sato, J., Kato, K., Hosseini, S.H.R., and Takayama, K. (2006), *Application of underwater shock wave and laser-induced liquid jet to neurosurgery*, Shock Waves, Vol. 15, pp. 55-67

Utsunomiya, Y., Kajiwara, T., Nishiyama, T., Nagayama, K., Kubota, S., and Nakahara, M. (2009), *Liquid Atomization Induced by Pulse Laser Reflection underneath Liquid Surface*, Japn J. Appl. Phys., Vol. 48 (2009) 052501-1-5.

Utsunomiya, Y., Kajiwara, T., Nishiyama, T., Nagayama, K. (2010), *Pulse laser ablation at water–air interface*, Appl. Phys. A, Vol.99, (2010) pp. 641–649.

Utsunomiya, Y. (2010a), *Laser ablation phenomena at liquid surface* [in Japanese], Doctorial Thesis, Kyushu University, 2010.

Vogel, A., and Venugopalan, V. (2003), *Mechanisms of Pulsed Laser Ablation of Biological Tissues*, Chem. Rev. (Wash. DC) Vol. 103, pp. 577-644

Watson, S., Gifford, M.J. Field, I.E. (2000), *The initiation of fine grain pentaerythritol tetranitrate by laser-driven flyer plates*, J. Appl. Phys. Vol. 88, pp. 65-

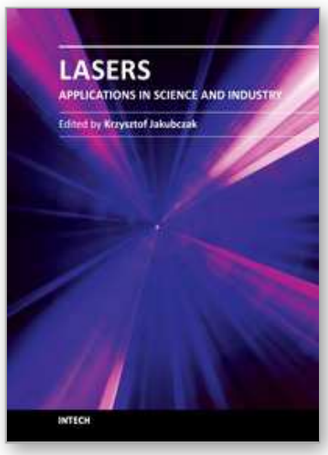

Lasers - Applications in Science and Industry
Edited by Dr Krzysztof Jakubczak

ISBN 978-953-307-755-0
Hard cover, 276 pages
Publisher InTech
Published online 09, December, 2011
Published in print edition December, 2011

The book starts with basic overview of physical phenomena on laser-matter interaction. Then it is followed by presentation of a number of laser applications in the nano-particles and thin films production, materials examination for industry, biological applications (in-vitro fertilization,tissue ablation) and long-range detection issues by LIDARs.

How to reference
In order to correctly reference this scholarly work, feel free to copy and paste the following:

Kunihito Nagayama, Yuji Utsunomiya, Takashi Kajiwara and Takashi Nishiyama (2011). Pulse Laser Ablation by Reflection of Laser Pulse at Interface of Transparent Materials, Lasers - Applications in Science and Industry, Dr Krzysztof Jakubczak (Ed.), ISBN: 978-953-307-755-0, InTech, Available from: http://www.intechopen.com/books/lasers-applications-in-science-and-industry/pulse-laser-ablation-by-reflection-of-laser-pulse-at-interface-of-transparent-materials

INTECH
open science | open minds

InTech Europe
University Campus STeP Ri
Slavka Krautzeka 83/A
51000 Rijeka, Croatia
Phone: +385 (51) 770 447
Fax: +385 (51) 686 166
www.intechopen.com

InTech China
Unit 405, Office Block, Hotel Equatorial Shanghai
No.65, Yan An Road (West), Shanghai, 200040, China
中国上海市延安西路65号上海国际贵都大饭店办公楼405单元
Phone: +86-21-62489820
Fax: +86-21-62489821

IntechOpen